

# Complex analysis of sea ice emission variability in the Sea of Okhotsk during transition period melting/freezing using passive/active microwave measurements

D.V. Darkin, and L. M. Mitnik

V.I. Il'ichev Pacific Oceanological Institute, Far Eastern Branch, Russian Academy of Sciences  
43 Baltiyskaya St., 690041, Vladivostok, Russia, - (dvdarkin, mitnik)@poi.dvo.ru

**Abstract** - The datasets of brightness temperatures  $T_B(\nu)$  over a range of frequencies  $\nu = 6.9 - 89$  GHz were obtained from AQUA AMSR-E (2002-2004) and from ADEOS-II AMSR (January-May 2003). At the same time, a large quantity of Envisat ASAR and ERS-2 SAR precision and quick-look images was acquired over the Okhotsk Sea. Sharp variations in day/night  $T_B(\nu)$  values of sea ice in winter and during the periods of ice melting caused by air temperature changes and the appearance of free water in the snow-sea-ice layer are investigated. Several case studies are used for detailed analysis. Variability properties in  $T_B(\nu)$  is compared with radar backscatter for the selected case studies. Collocated surface analysis maps are used to support the analysis. The results are discussed and directions for further research are outlined.

**Keywords:** sea ice, Okhotsk Sea, Aqua AMSR-E, ADEOS-II AMSR, Envisat ASAR, melting/freezing, ice concentration algorithms.

## 1. INTRODUCTION

Meteorological and oceanic characteristics of the Okhotsk Sea are close to those of the polar ocean. They include severe winters with low air temperature and enhanced cyclone activity, extended period of ice cover, etc. Gale winds accompanying cyclones and convective atmospheric vortices significantly influence the formation, development of ice cover, and the position and structure of the ice edge. From this follows the need of gaining operational information about ice cover and surface wind characteristics. In turn, this information is essential for solving scientific problems, in particular those involving ice margin processes (water mass formation, oceanic upwelling, eddy formation, etc.), synoptic and mesoscale processes in the atmosphere including instability generation, air-sea-ice interaction.

In this study, the possibility of monitoring freeze/thaw cycles using passive and active microwave data collected by the AMSR and AMSR-E radiometers flown onboard of the ADEOS-II and Aqua satellites, Advanced Synthetic Aperture Radar (ASAR) flown onboard of the European Envisat satellite is investigated.

The expected merits of using the passive/active microwave data are:

- In the microwave range the sea ice can be observed independently on sun illumination and cloudiness.
- Due to combination of the broad swath twice per day low resolution of the radiometers (passive) and scatterometer (active) instruments and scarce high resolution SAR (active) data freeze/thaw cycles can be investigated in details at an

adequate scale and a technique for their monitored can be developed.

- Algorithms for sea ice classification and ice concentration estimate can be improved.

The purpose of a given work is an estimation of the variability the sea ice characteristics during winter and spring seasons. Special attention is given to detailed consideration of freezing/melting process.

## 2. DATA AND PHYSICAL PRINCIPLES

Winter season 2003 was very special in terms of passive microwave remote sensing data availability. During this period ADEOS-II AMSR data complimented measurements of Aqua AMSR-E. This resulted in a large dataset of calibrated brightness temperatures  $T_B^{V,H}(\nu)$  at  $\nu = 6.9, 10.65, 18.7, 23.8, 36.5, 89.0$  GHz with vertical (V) and horizontal (H) polarization. For example during February - April 2003 there were twice as many swaths providing possibility to study variations of microwave characteristics of ice cover on a finer time scale.

Detailed regional ice studies can be carried out with the high resolution (10-150 m) satellite SAR. Information on ice cover for the whole Okhotsk Sea can be obtained with the Envisat ASAR operating at the wavelength  $\lambda = 5.6$  cm at V- or H-polarization using a wide swath (405 km) regime at a ground resolution of 150 m.

In principle, two groups of the underlying surface parameters can be separated influencing the microwave emissivity and backscatter behavior of natural media, geometric and physical ones. Geometric parameters include for example the surface roughness, the shape and the orientation of large structure elements. Changes of these parameters result in a change between the amount of mirror, diffuse and volume scattering, consequently changing the brightness temperatures  $T_{BS}$  and normalized radar cross section  $\sigma^\circ$ .

Short term variations of  $T_{BS}$  and  $\sigma^\circ$  are therefore indicators for the dielectric permittivity  $\epsilon(\nu)$  of the observed surface patch determining its emissivity/backscatter and also a depth of penetration of electromagnetic waves. Changes of the  $\epsilon(\nu)$  are tightly linked to changes of the moisture content of the uppermost snow-ice layer which is influenced by melting/freezing cycles, precipitation, splashing and flooding. As opposite to  $T_{BS}$ ,  $\sigma^\circ$  is not related to the sea ice temperature but to physical parameters that are temperature driven (Carsey, 1992). The interpretation of  $T_{BS}$  should be based on evolution of snow/ice thermophysical properties, including water in the liquid phase present in the system, snow pack density, and snow grain metamorphism.

## 2. PROCESSING OF BRIGHTNESS TEMPERATURES

In order to examine variability of diurnal changes in brightness temperatures across common AMSR/AMSR-E channels two datasets were processed. Initial processing and dataset preparation involved gridding of data and land masking. All channels except 89 GHz V-pol and H-pol were gridded on 10 x 10 km regular grid and 89 GHz V-pol and H-pol channels were gridded on 3.5 x 3.5 km regular grid. Land was masked for the whole area of the Okhotsk Sea which was bound by 42-60°N and 137-160°E.

The first dataset consisting of measurements of ADEOS-II AMSR and Aqua AMSR-E during February – March 2003 and the second dataset consisting of Aqua AMSR-E measurements during March 2004 were processed in the same manner. Differences  $\Delta T_B(v)$  between night and day acquisitions were prepared. To detect the maximum  $T_B$  changes in AMSR/AMSR-E measurements, night swaths falling within a range 3-7 A.M. and day swaths falling within 1-7 P.M. the Okhotsk Sea local time (+ 11 UTC) were selected to take into account a shift between the maximum/minimum diurnal temperatures and maximum/minimum ice melting/freezing (Harouche and Barber, 2001).

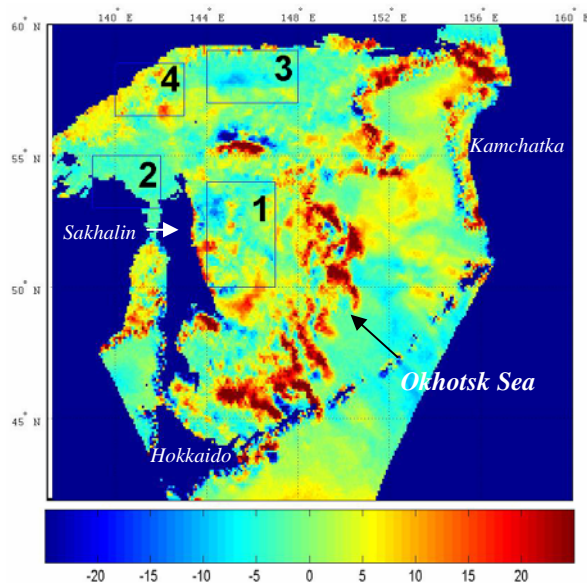


Figure 1. Difference frame of brightness temperatures  $T_B(19H)$  acquired by Aqua AMSR-E on 20 February 2003 at 16:45 UTC (night swath) and at 02:45 UTC (day swath). The colour scale displays  $T_B(19H)$  changes of in K

Creation of difference frames between night and day swaths lead to a somewhat sparse time series with gaps of several days between the difference frames mainly due to the fact that day and night swaths were selected to maximize the changes in brightness temperatures.

Out of prepared time series where each difference frame covers the whole Okhotsk Sea, several smaller areas were selected for detailed analysis. This was done based on the oceanographic and sea ice distribution features summarized in (Gluchovskiy et al., 2003) in order to select regions which

differs in of sea ice types and dynamics. Difference frame between the descending night swath (16:45 UTC) and ascending day swath (02:45 UTC) acquired on 20 February 2003 is presented in Figure 1. An narrow indented band characterized by  $\Delta T_B(v) > 20$  K and crossing the whole Okhotsk Sea marks the area of new ice formation during 14 h. Four regions of the study are outlined and numbered in boxes.

The first region (50-54°N, 144°-147°E) is located along the Sakhalin coast at in the area of the East Sakhalin Current and was chosen as dynamic area. This region is characterized by almost constant openings of ice cover that form streaks of hundreds of kilometres along the coast.

The second region (53-55.5°N, 139-142°E) covers the Sakhalin Bay and its surroundings and is characterized by the presence of fast ice and medium first-year ice with ice concentration  $> 90\%$ . This region was selected in order to study the variability of microwave properties of sea ice which is not drastically affected by oceanic factors.

The third region (57-59°N, 144-148°E) is located to the north of Kashevarova Bank. White ice and medium first-year ice with concentration 70-100 % was usually prevailed here impacted by both oceanic and atmospheric conditions.

The fourth region (56.5-58.5°N, 140-143°E) located near the north-west coast of the Okhotsk Sea can be described as ice factory. Here winds from the continent often drag the ice towards the open sea and cold air temperatures account for fast formation of new ice forms in open water areas.

The average  $\Delta T_B(v)$  values and dispersions were computed for all differences for each region and histograms showing distribution of  $\Delta T_B(v)$  pixels were constructed. These quantitative characteristics in combination with  $\Delta T_B(v)$  colour images gave more clearly idea on the homogeneity of each regions as a function of time as well as on change of the homogeneity under influence of weather conditions.

## 4. TIME SERIES OF BRIGHTNESS TEMPERATURE DIFFERENCES CASE STUDIES

In the time series of microwave observations, covering February - April 2003 three distinct periods can be revealed differing in diurnal changes of brightness temperatures. During February stable growth of ice cover was observed and diurnal changes of  $T_Bs$  were determined by the changes of the underlying surface temperature. At the end of February and in March amplitude of diurnal changes substantially increased due to the increase of wetness of the uppermost layer caused by thawing. In April the amount of free water increased and ice cover was exposed to severe deterioration. It was accompanied by the significant variations of brightness temperature which were different for selected regions.

### 4.1 February 2003. Stable ice growth

During February 2003 ice cover development was rapid which is well explained by low air temperatures and several cold air outbreaks from north-western coast (Darkin et. al., 2004). Figure 2 shows advancement of ice cover in February 2003. Two black contours labelled 1 and 2 depict the position of ice edge on 3 February and 27 February, respectively. The area of the ice cover of the Okhotsk Sea constituted around 1 580 000 km<sup>2</sup> on 3 February, whereas on 27 February the ice cover extended to the area of around 1 870 000 km<sup>2</sup>.

It is necessary to note that the computed ice cover area included not only the Okhotsk Sea but also the Tartar Strait in the Japan Sea and ice along the east Kamchatka coast bound by selected quadrant of (42-60°N, 137-160°E). The pixel values of 10 x 10 km gridded  $T_B(19H)$  dataset that are above 120 K were marked as containing ice. Sobel edge detection filter was used to generate the ice edge (Figure 2).

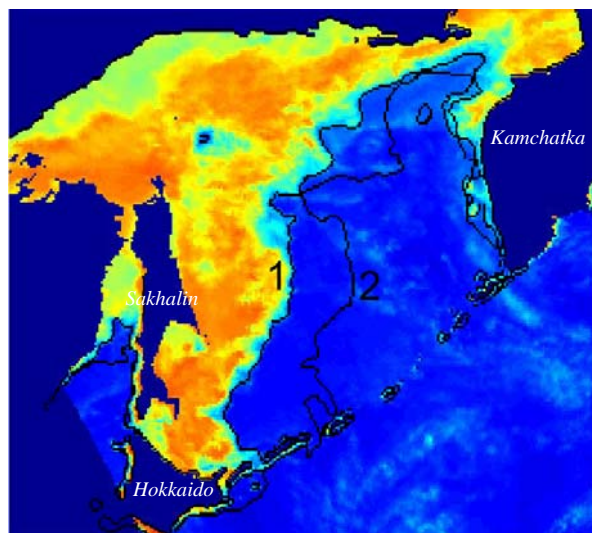


Figure 2. Advancement of ice edge overlaid on  $T_B(19H)$  taken by ADEOS-II AMSR on 3 February 2003 at 11:28 UTC. Ice edge location: (1) - 3 February and (2) - 27 February.

Variations of  $T_B$ s for two differences are presented in Table 1. The first difference is between day (9 February at 03:35 UTC) and night (8 February at 16:21 UTC) swaths. The second one is between night (17:04 UTC) and day (03:35 UTC) swaths on 9 February. It can be seen that differences are not very pronounced and are due to diurnal thermodynamic temperature changes in the snow-sea-ice layer.

Table 1. Dates ( $d$  – day,  $n$  – night), diurnal air temperatures and  $\Delta T_B$  (Kelvin degrees) changes for AMSR/AMSR-E channels over selected regions in February 2003.

Date – Date	$^{\circ}C_{air}$	6.9 (V,H)	10.6 (V,H)	18.7 (V,H)	23.8 (V,H)	36.5 (V,H)	89.0 (V,H)
Region 1							
09 d	-12	0.7	-0.1	1.5	1.6	2.0	-1.7
08 n	-15	-0.3	-0.2	1.8	-0.5	1.7	-3.3
09 n	-14	1.9	1.9	0.2	-0.1	-1.1	0.8
09 d	-12	2.5	3.0	-0.6	1.3	-1.8	0.8
Region 2							
09 d	-8	1.5	-0.3	1.0	1.6	2.3	-0.1
08 n	-15	1.2	-0.3	3.0	1.23	2.9	-1.0
09 n	-10	-0.1	0.3	-1.4	-1.6	-2.4	-0.3
09 d	-8	1.0	1.2	-2.8	-1.3	-3.0	0.3
Region 3							
09 d	-13	1.6	1.0	2.5	2.4	1.9	-3.0
08 n	-13	2.2	2.4	5.1	2.9	3.5	-2.4
09 n	-15	2.5	2.1	-0.3	-1.0	-3.0	-0.6
09 d	-13	4.9	4.3	-0.4	0.5	-1.8	0.4

Region 4							
09 d	-16	0.2	-2.0	-1.0	-0.4	0.3	-2.9
08 n	-19	-4.4	-5.9	-2.0	-3.7	-0.9	-4.7
09 n	-22	1.5	2.1	0.9	1.7	-0.3	2.0
09 d	-16	3.4	3.9	0.3	-0.3	-1.3	2.6

It can also be noted that as the difference pair moves from day – night to night – day, the signs of the  $T_B$ s do change across frequency channels, but there are some exceptions as well. Some of the changes in the  $T_B$ s can be related to regional oceanographic features of the Okhotsk Sea. As an example of this a  $\Delta T_B$  difference frame is compared with a fragment of Envisat ASAR image (Figure 3). It is clearly visible that the areas of most positive  $\Delta T_B$  changes correspond to inhomogeneous streak-like structures which are characterized by reduced brightness (radar backscatter) on ASAR image (Figure 3a). These changes could be related to formation of new ice in the quasi-constant opening along the Sakhalin coast during day – night transition.

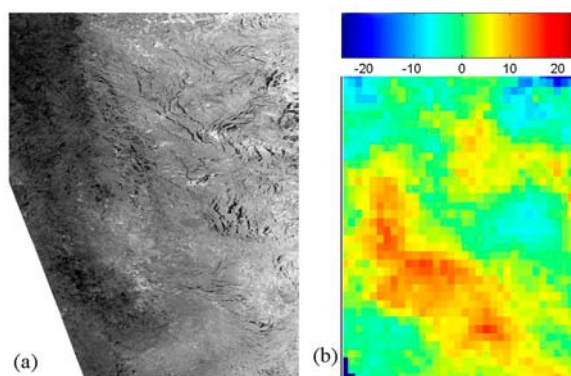


Figure 3. Fragment of Envisat ASAR image at V-pol at 11:52 UTC (a) and  $\Delta T_B(19H)$  between 16:21 UTC and 02:20 UTC (b) on 8 February 2003. Colour scale in Kelvin degrees.

#### 4.2 March 2003. Increase of diurnal freeze/thaw processes

From the analysis of March 2003 time series it can be concluded that in March variability of  $\Delta T_B$  increased. The region 2 was the least variable whereas region 3 showed the most dramatic amplitude changes in diurnal  $\Delta T_B$ . Some data outlining the diurnal changes of  $\Delta T_B$  is given in Table 2.

Table 2. Dates ( $d$  – day,  $n$  – night), diurnal air temperatures and  $\Delta T_B$  (Kelvin degrees) changes for AMSR/AMSR-E channels over selected regions in March 2003.

Date – Date	$^{\circ}C_{air}$	6.9 (V,H)	10.6 (V,H)	18.7 (V,H)	23.8 (V,H)	36.5 (V,H)	89.0 (V,H)
Region 1							
10 n	-18	-1.6	-1.6	-2.3	-1.6	-2.4	0.2
10 d	-10	-0.2	-0.8	-1.2	1.9	-0.5	4.6
16d	-6	-1.6	0.1	1.6	1.3	2.1	3.6
15n	-6	-1.5	1.1	3.1	0.4	0.5	3.7
17 n	-4	0.8	-1.4	-4.2	-3.8	-4.7	-5.4
17 d	-7	4.1	-1.5	-5.7	-3.5	-4.4	-4.5
Region 2							

10 n	-16	0.9	0.8	0.0	0.1	-0.6	-0.4
10 d	-22	1.4	1.0	-0.9	0.2	-1.8	-0.5
16 d	-18	1.2	1.3	2.2	2.0	3.5	6.8
15 n	-22	0.8	1.7	3.7	2.0	4.0	7.1
17 n	-21	-1.0	-1.1	-2.3	-1.9	-3.7	-7.5
17 d	-16	-0.3	-1.0	-3.3	-3.7	-4.0	-7.0
Region 3							
10 n	-9	-2.4	-1.4	-2.1	-1.0	-0.9	4.8
10 d	-10	-7.1	-7.5	-8.1	-5.2	-6.1	2.8
16 d	-9	-1.4	0.0	1.5	1.1	2.1	3.2
15 n	-8	-1.9	0.1	3.0	1.5	2.8	3.1
17 n	-10	3.2	2.2	0.1	-0.1	-1.9	-7.0
17 d	-8	7.1	5.8	2.7	3.0	0.0	-6.2
Region 4							
10 n	-7	-1.1	-1.2	-2.1	-1.9	-1.8	0.4
10 d	-10	-7.8	-8.9	-9.1	-6.5	-7.3	-3.1
16 d	-6	-4.6	-3.3	-1.0	-0.6	1.1	2.0
15 n	-8	-10.0	-8.2	-5.1	-5.5	-1.9	-0.6
17 n	-10	4.5	3.6	1.6	1.4	-0.4	-1.6
17 d	-10	8.5	8.6	7.0	7.7	4.2	1.3

### 4.3. April 2003. Rapid deterioration of ice cover

Time series of microwave observations in April exhibits very drastic variations of  $\Delta T_B(v)$  across all channels. Regions 1, 3 and 4 due to their location had to be excluded from the analysis on a rather early stage of April because of large open water areas. The most persistent region which is region 2 still had very severe changes in day-night, night-day differences that increased from up to  $\pm 10$  K in the beginning of April to up to  $\pm 30$  K by the 19<sup>th</sup> of April 2003. Figure 4a shows region 2 on April 12 as seen by Envisat ASAR and corresponding Figure 4b displays the difference between 17:16 UTC and 03:15 UTC on 12 April. Polynia is visible on ASAR fragment suggesting that ice destruction started in the most stable ice region of current analysis.

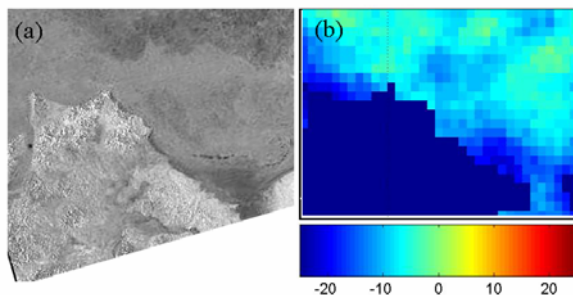


Figure 4. Close pack ice and fast ice in the Sakhalin Bay on Envisat ASAR image at UTC (a) and  $\Delta T_B(19H)$  between 17:16 UTC and 3:15 UTC on 12 April (b). Colour scale in Kelvin degrees.

### 5. CONCLUSIONS

Microwave brightness temperatures as well as backscatter signals are the good indicators for defining evolution of snow/ice cover in the Okhotsk Sea. Time series of  $T_B$ s can be used successfully in collocation of other remotely sensed data to obtain quantitative and qualitative results about ice cover

development and it's relation to atmospheric and oceanic processes. Looking at the Figure 5. drawn to illustrate preliminary conclusions of this research we can mention that the overall amplitude of  $\Delta T_B$  across all channels tends to increase as time series progress to April. The amplitudes in H-pol channels are more pronounced. Average level of  $\Delta T_B$  at 89.0, 36.5 and 23.8 GHz with H-polarization seems to shift toward negative values as times series progress to April that can be explained by the appearance of melt ponds. Further research is needed involving more *in situ* and remote sensing data such as Aqua/Terra MODIS data, QuikSCAT SeaWinds data and NOAA AVHRR visible and infrared images.

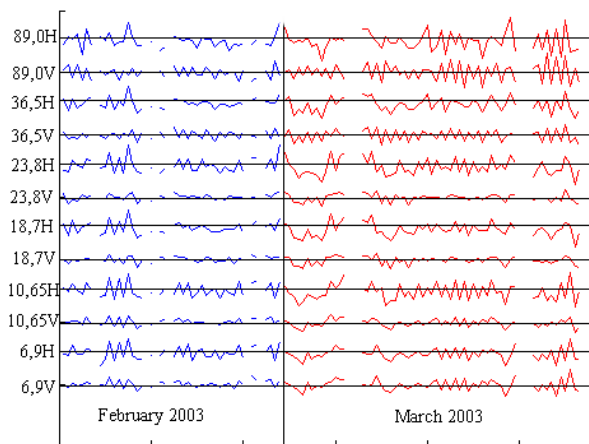


Figure 5. Mean changes of  $\Delta T_B$  of Region 3 across all AMSR/AMSR-E channels for February and March 2003.

### 6. ACKNOWLEDGEMENTS

This study has been carried out within the cooperation between the Japan Aerospace Exploitation Agency and the POI FEB RAS in the ADEOS-II Research activity (project A2ARF006) and within ESA Envisat project AO-ID-391: "Study of the interaction of oceanic and atmospheric processes in the Japan Sea and the Southern Okhotsk Sea". This work is partially sponsored by grants for projects "Investigation of variability and structure of the ice cover of the Sea of Okhotsk with usage of remote sensing data from Aqua, ERS-2, Envisat and Sich - 1M" and "Investigation of ocean-atmosphere system with passive and active microwave sensing from new generation satellites" from Far Eastern Branch of the Russian Academy of Sciences.

### 7. REFERENCES

- F.D. Carsey, (Editor), "Microwave Remote Sensing of Sea Ice." Geophysical monograph 68. 462 pp. 1992.
- J.C. Comiso, "AMSR-E / AMSR Sea Ice Algorithm." Paper presented at ADEOS-II PI workshop, Nagahama, Japan, 8-10 December 2004. 2004.
- D.V. Darkin, L.M. Mitnik, and V.A. Dubina "Ice cover of the Okhotsk Sea: a study using ENVISAT ASAR, ERS-2 SAR and AQUA AMSR-E data," Envisat & ERS ESA Symposium (Austria, 2004), ESA SP-572 Publication, 7 pp (in press).
- Harouche I. P.-F., and D.G. Barber, "Seasonal characterization of microwave emission from snow-covered first-year ice," Hydrol. Process., vol. 15, p.p. 3571-3583, 2001.
- Gluchovskiy B., Goptarev N., and Terziev F. Eds., Ice conditions and methods for prognosis, Sea Hydrometeorology and Hydrochemistry, Vol. IX, Okhotsk Sea, Hydrometeoizdat, 1998 (in Russian).